

CONFIDENTIAL



RESEARCH MEMORANDUM

SUMMARY OF SOME ROCKET-MODEL INVESTIGATIONS OF EFFECTS OF
WING ASPECT RATIO AND THICKNESS ON AILERON ROLLING
EFFECTIVENESS INCLUDING SOME EFFECTS OF SPANWISE
AILERON LOCATION FOR SWEEPBACK WINGS

WITH ASPECT RATIO OF 8.0

By H. Kurt Strass

Langley Aeronautical Laboratory
Langley Field, Va.

CLASSIFIED DOCUMENT

This material contains information affecting the National Defense of the United States within the meaning of the espionage laws, Title 18, U.S.C., Secs. 793 and 794, the transmission or revelation of which in any manner to an unauthorized person is prohibited by law.

NATIONAL ADVISORY COMMITTEE FOR AERONAUTICS

WASHINGTON

February 17, 1954

CONFIDENTIAL

CLASSIFICATION CHANGED TO UNCLASSIFIED

AUTHORITY: NACA RESEARCH ABSTRACT NO. 111

EFFECTIVE DATE: JANUARY 10, 1957

WHI

NATIONAL ADVISORY COMMITTEE FOR AERONAUTICS

RESEARCH MEMORANDUM

SUMMARY OF SOME ROCKET-MODEL INVESTIGATIONS OF EFFECTS OF
WING ASPECT RATIO AND THICKNESS ON AILERON ROLLING
EFFECTIVENESS INCLUDING SOME EFFECTS OF SPANWISE
AILERON LOCATION FOR SWEEPBACK WINGS
WITH ASPECT RATIO OF 8.0

By H. Kurt Strass

SUMMARY

The rolling effectiveness of 0.2-chord, trailing-edge ailerons on high-aspect-ratio sweptback wings over a Mach number range of 0.6 to 1.6 has been investigated by the Langley Pilotless Aircraft Research Division by utilizing rocket-propelled test vehicles in free flight. Some effects of spanwise aileron location on rolling effectiveness were measured by testing ailerons on the inboard half, the outboard half, and the full length of the exposed wings. The test wings had NACA 65₁A012 airfoil sections, an aspect ratio of 8.0, 45° sweepback of the midchord line, and taper ratios of 0.5 and 1.0. In addition, these data are correlated with the results of previous investigations of various plan forms to show some effects of wing aspect ratio and airfoil section thickness ratio.

The results show that all of the aileron configurations when used on 12-percent-thick wings with an aspect ratio of 8.0 were subject to severe losses in rolling effectiveness and aerodynamic reversal at Mach numbers between approximately 1.0 and 1.4. The correlation with previous data indicates that, in general, increasing the aspect ratio and the airfoil thickness resulted in decreased aileron rolling effectiveness throughout the speed range tested.

INTRODUCTION

A general investigation of the rolling effectiveness of wing-aileron configurations is being conducted by the Langley Pilotless Aircraft

Research Division by utilizing rocket-propelled test vehicles in free flight at transonic and supersonic speeds. In continuance of this program, a limited investigation of the rolling effectiveness of 0.2-chord, trailing-edge ailerons on sweptback wings of high aspect ratio has been completed. These data are correlated with the results of previous investigations to show some effects of aspect ratio and airfoil thickness ratio on rolling effectiveness. In addition, some effects of spanwise aileron location on the high-aspect-ratio wings were measured by testing ailerons on the inboard half, the outboard half, and the full length of the exposed wings.

SYMBOLS

A	aspect ratio, b^2/S
b	diameter of circle swept by wing tips, ft
c	wing chord measured parallel to model center line, ft
c_a	aileron chord, ft
E	Young's modulus of elasticity, lb/sq in.
G	shear modulus of elasticity, lb/sq in.
i_w	average wing incidence for three wings, measured in a plane parallel to model center line, deg
I	local moment of inertia of airfoil cross section parallel to model center line about chord plane, in. ⁴
J	local torsional-stiffness constant of airfoil cross section in a plane parallel to model center line, in. ⁴
EI	flexural-stiffness parameter of streamwise airfoil cross section, lb-in. ²
GJ	torsional-stiffness parameter of streamwise airfoil cross section, lb-in. ²
$\frac{c^4}{GJ}$	nonscalar torsional-stiffness constant, sq in./lb
M	free-stream Mach number

p	test-vehicle rolling velocity, radians/sec
q	dynamic pressure, lb/sq ft
R	Reynolds number based on average wing chord
S	area of two wings taken to fuselage center line, sq ft
t	maximum local wing thickness, ft
$pb/2V$	wing-tip helix angle, radians
V	flight-path velocity, ft/sec
δ_a	average aileron deflection for three wings, measured in a plane perpendicular to chord plane and parallel to model center line, deg
λ	ratio of tip chord to extended chord at model center line
Λ	angle of sweep measured at $c/2$, deg
α_δ	control-effectiveness parameter, effective change in wing angle of attack caused by unit change in aileron deflection
C_{L_α}	wing lift-curve slope
C_l	rolling-moment coefficient, positive clockwise when viewed from rear, $\frac{\text{Rolling moment}}{qSb}$
$C_{l_\delta} = \frac{\partial C_l}{\partial \delta}$	
$C_{l_p} = \frac{\partial C_l}{\partial \frac{pb}{2V}}$	

MODELS AND TECHNIQUE

Photographs of typical test vehicles are presented in figure 1, the general arrangement of the test vehicles is presented in figure 2, and the geometry and dimensions of the test wings are given in figure 3. The

structural and geometrical parameters are presented in table I. The test wings, which were built up of wood and metal, are referred to as being of "composite" construction. A typical example of this type of construction is presented in figure 4. Wings of composite construction are somewhat stiffer in bending than solid metal wings of equal torsional stiffness so that this type of construction is particularly advantageous for use with swept wings, where wing bending is the predominant cause of aeroelastic effects, as opposed to unswept wings, where wing twisting is the primary cause of aeroelastic effects. In table I, the values of c^4/GJ denote the torsional stiffness and GJ/EI the ratio of the torsional stiffness to the bending stiffness. Both values are independent of wing size or scale and, in the case of tapered wings, represent the structural characteristics at the mean exposed chord. It should be noted that the values of EI and GJ were computed according to the method used in reference 1.

The flight tests were made at the Pilotless Aircraft Research Station at Wallops Island, Va. The test vehicles were propelled to supersonic speeds by a two-stage rocket-propulsion system. During a 12-second period of coasting flight following rocket-motor burnout, time histories of the rolling velocity were obtained with special radio equipment (spin-sonde) and the flight-path velocity was obtained by the use of CW Doppler radar. These data, in conjunction with atmospheric data obtained with radiosondes, permit the evaluation of the aileron rolling effectiveness in terms of the parameter $pb/2V$ as a function of Mach number.

Figure 5 presents the average variation of Reynolds number and dynamic pressure with Mach number for the models discussed in this paper.

ACCURACY

From previous experience and mathematical analysis it is estimated that the experimental error is within the following limits:

	Subsonic	Supersonic
$pb/2V$, radians	± 0.004	± 0.002
M	± 0.01	± 0.005

DATA CORRECTIONS AND REDUCTION

All of the data have been corrected to nominal values of $i_w = 0^\circ$ and $\delta_a = 5.0^\circ$. The corrections in all cases were relatively small and consisted of adjusting the data for the effects of normal constructional

tolerances. Incidence errors were corrected by the method of reference 2 and aileron-deflection errors were corrected by reducing the data to $\frac{pb/2V}{\delta_a}$ and then multiplying by the nominal δ_a value of 5.0° .

No attempt was made to correct for the effects of test-vehicle moment of inertia about the roll axis on the measured variation of $pb/2V$ with Mach number since previous experience has demonstrated that the effects are within the accuracy of measurement.

All of the data have been corrected for the effects of aeroelasticity by the method presented in reference 1. The data are presented two ways:

- (1) Corrected to rigid-wing values
- (2) Corrected to solid-aluminum-alloy values

Rigid-wing data are presented in order to show the aerodynamic behavior free from the effects of aeroelasticity. However, in many practical cases, aeroelastic effects are quite important and for this reason the data are also presented corrected to solid-aluminum-alloy values which more nearly approximate the construction of wings planned for use at supersonic speeds. It should be noted here that approximately one-half of the data were obtained from models which were of composite construction (see table I). The magnitude of the aeroelastic correction involved in converting the data from the composite construction to the solid-aluminum-alloy case was small in all instances.

The data for configuration 1 (see table I) were first published in reference 3 where the models were referred to as 57(a) and 57(b). These models were indicated as having $A = 1.75$ and NACA 65-009 airfoil sections; however, the apparent discrepancy in the magnitude of A (now given as $A = 2.3$) results from differing definitions of A . In addition, the airfoil section, while labeled NACA 65-009, actually, as it was later discovered, closely approximated the NACA 65A009 section because of a relatively thick layer of paint which filled in the cusped trailing-edge portion of the NACA 65-009 section. The data for the bastard section were then corrected to the NACA 65A009 section by use of reference 4. Only a small correction in the transonic region was necessary because the trailing-edge angle of the bastard section was very close to that of the NACA 65A009 section.

The lack of aerodynamic data applicable to the $A = 8.0$ wings above $M \approx 0.9$ made it necessary to use certain assumptions regarding the wing lift-curve slope C_{L_α} and the control effectiveness α_δ in order to correct the data for the effects of wing flexibility by the method of reference 1.

For a rigid wing,

$$\frac{pb/2V}{\delta_a} = \frac{C_{l\delta}}{C_{lp}}$$

$$= \frac{\alpha_\delta \int_{x_1}^{x_2} c_{l\alpha_1} cx \, dx}{\frac{2}{b} \int_0^{b/2} c_{l\alpha_2} cx^2 \, dx}$$

where

- x spanwise location
 x₁ spanwise location of inboard end of aileron
 x₂ spanwise location of outboard end of aileron
 c_{lα₁}, c_{lα₂} section lift-curve slopes

But at any point along the span,

$$c_{l\alpha_1} \approx c_{l\alpha_2}$$

Then

$$\frac{pb/2V}{\delta_a} = \frac{\alpha_\delta \int_{x_1}^{x_2} cx \, dx}{\frac{2}{b} \int_0^{b/2} cx^2 \, dx}$$

$$= \alpha_\delta K$$

Therefore, α_δ was estimated by extrapolating existing wind-tunnel data by assuming that, for a rigid wing, α_δ is proportional to pb/2V. This

assumption, when applied to flexible-wing data, required that α_δ be obtained by iteration. However, the initial values of α_δ obtained by this method were low and the absolute magnitude of the change in $pb/2V$ due to aeroelasticity in the supersonic region was so small that it was not necessary to make more than two iterating steps in any case.

The lift-curve slope C_{L_α} was obtained by extrapolating existing wind-tunnel data with the aid of linearized theory (ref. 5). The aeroelastic corrections for the configurations of lower aspect ratio were based upon interpolated wind-tunnel data.

RESULTS AND DISCUSSION

Two examples of the effect of wing flexibility upon the aileron rolling effectiveness are presented in figure 6. These data, except for configuration 20, were originally published in reference 1 and are presented here to illustrate the order of magnitude of the aeroelastic corrections. It should be noted that correction of the data to rigid-wing values did not materially alter the nature of the variation of $pb/2V$ with M in the supersonic region. The following discussion applies to the rigid-wing values unless otherwise noted.

Figures 7 and 8 present some effects of aileron location upon the aileron rolling effectiveness for the 12-percent-thick wings with $A = 8.0$. The results for the untapered and the tapered wings are essentially the same. In the subsonic region the outboard ailerons were slightly more effective than the inboard ailerons for the rigid-wing case and slightly less effective or approximately equal to the inboard ailerons for the solid-aluminum-alloy wings. In the supersonic region, all of these data were characterized by an extremely low level of rolling effectiveness, with either a complete loss or a reversal of rolling effectiveness occurring near $M \approx 1.1$. Above $M \approx 1.4$, all of the ailerons exhibited varying degrees of effectiveness recovery.

Figures 9 to 14 present several correlations which show some effects of aspect ratio and airfoil thickness upon the variation of $pb/2V$ with Mach number for unswept and 45° sweptback wings employing full-span ailerons.

The effects of aspect ratio are presented in figures 9, 10, and 11. For the rigid-wing cases they are similar, with a few exceptions, for both the unswept and sweptback wings. Large decreases in $pb/2V$ occur with increasing aspect ratio throughout most of the supersonic region, whereas, the effect of aspect ratio is not as well defined below $M \approx 1.0$. In general, the data for the 9-percent-thick unswept wings presented in

figure 9(a) indicate that the largest decreases in effectiveness with increasing aspect ratio occur at low aspect ratios for both subsonic and supersonic speeds, whereas, for sweptback wings, the data presented in figure 10(a) indicate that only a general decrease occurs with increasing aspect ratios. Figure 11 shows the effect of changing the aspect ratio for the 12-percent-thick sweptback wings. In this case no significant effect is apparent in the subsonic range, but in the region between $M \approx 1.0$ and $M \approx 1.4$, the effectiveness decreased markedly with increasing speed, until at $M \approx 1.1$ complete reversal is experienced for the wing with $A = 8.0$. Above $M \approx 1.4$, the high-aspect-ratio wing has apparently regained rolling effectiveness equal to that of the wing with $A = 3.7$.

Figure 12 illustrates the effect of airfoil thickness ratio upon the aileron rolling effectiveness for the unswept wings with $A = 3.7$. Increasing the thickness ratio had a very pronounced effect throughout most of the speed range above $M \approx 0.80$ in that increased thickness resulted in decreased effectiveness. This effect was greatly exaggerated near $M \approx 0.9$ and resulted in complete control reversal for the 12-percent-thick wing. Reference 4 indicates that the primary cause of the deterioration in rolling effectiveness which takes place with the thicker airfoil sections is the increased trailing-edge angle of the thicker sections. The 3-percent-thick solid-aluminum-alloy wings exhibited severe losses of rolling effectiveness throughout the speed range as a result of wing flexibility and underwent reversal of rolling effectiveness at $M = 1.27$.

Figures 13 and 14 show the effects of increasing the thickness ratio upon the aileron rolling effectiveness for the sweptback wings with aspect ratios of 3.7 and 8.0. The data presented in figure 13 show that no appreciable change in rolling effectiveness was caused by increasing the thickness ratio from 6 percent to 9 percent for the low-aspect-ratio wings; however, a further increase to 12 percent resulted in a marked loss of control throughout the entire speed range. The effect of changing the thickness ratio from 9 to 12 percent for the wings with $A = 8.0$ is remarkably similar to the effect of aspect ratio as given in figure 11. This similarity between the effects of aspect ratio and thickness is illustrated in figure 15, where the rigid $pb/2V$ values for the unswept wings at $M = 1.0$ are plotted against $A\left(\frac{t}{c}\right)^{1/3}$, one of the parameters commonly used in the application of the transonic similarity rules. The correlation is good and, at values of $A\left(\frac{t}{c}\right)^{1/3} \approx 1.6$ and higher, little additional change in $pb/2V$ is evident. The abrupt change which occurs in the slope of the faired correlation curve at $A\left(\frac{t}{c}\right)^{1/3} \approx 1.6$ is fairly typical of some other aerodynamic parameters which have been correlated in this manner (see ref. 6). For comparison, calculated values of $pb/2V$

at the limiting values of $A\left(\frac{t}{c}\right)^{1/3}$ are presented. The value at $A\left(\frac{t}{c}\right)^{1/3} = 0$ was calculated by using values of C_{l_δ} and C_{l_p} presented in reference 7. The strip-theory values were calculated by assuming that C_{l_δ} is proportional to c_a/c .

CONCLUDING REMARKS

The test data presented in this paper demonstrate that for the rigid-wing cases the effects of aspect ratio and thickness ratio upon the aileron rolling effectiveness are similar in many respects. For example: the data for the unswept wings indicate that the rolling effectiveness decreases with increasing aspect ratio, the effect being somewhat less at subsonic speeds than at supersonic speeds. The greatest effect of aspect ratio apparently occurs at low aspect ratios. Similarly, the effect of airfoil thickness ratio is greatest at supersonic speeds and negligible at speeds below a Mach number of about 0.8.

The data for the swept wings show that the effect of aspect ratio is apparently only a general decrease of rolling effectiveness with increasing aspect ratio. Similarly, the greatest effect of thickness ratio occurred at the highest values of thickness ratio, with the proportionally largest decrease occurring at supersonic speeds.

Obviously, this comparison is limited, but it serves to illustrate the extremely poor rolling effectiveness which was experienced by the various configurations that had 12-percent-thick wings with an aspect ratio of 8.0. In these instances, the deleterious effects of high aspect ratio and high airfoil thickness ratio are superimposed.

Langley Aeronautical Laboratory,
National Advisory Committee for Aeronautics,
Langley Field, Va., November 24, 1953.

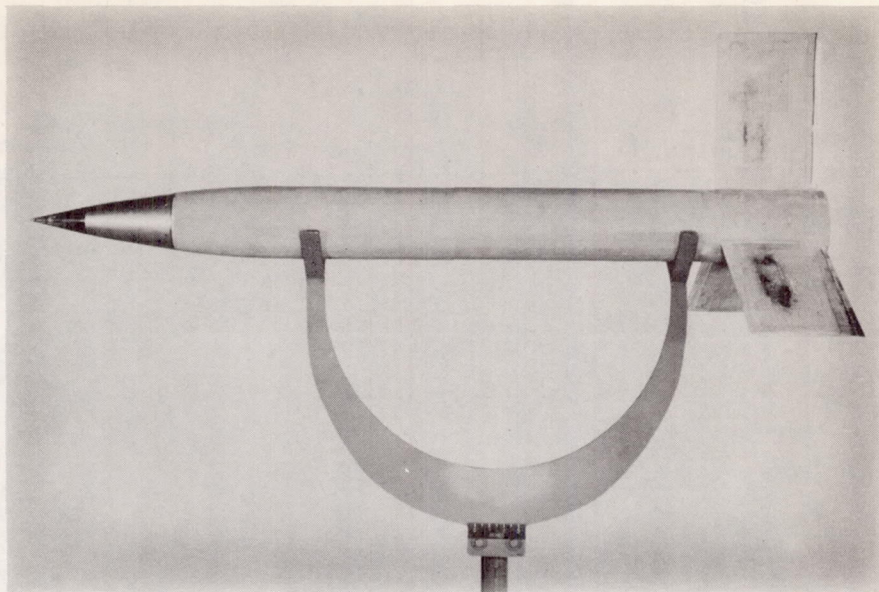
REFERENCES

1. Strass, H. Kurt, and Stephens, Emily W.: An Engineering Method for the Determination of Aeroelastic Effects Upon the Rolling Effectiveness of Ailerons on Swept Wings. NACA RM L53H14, 1953.
2. Strass, H. Kurt, and Marley, Edward T.: Rolling Effectiveness of All-Movable Wings at Small Angles of Incidence at Mach Numbers From 0.6 to 1.6. NACA RM L51H03, 1951.
3. Sandahl, Carl A.: Free-Flight Investigation of Control Effectiveness of Full-Span, 0.2-Chord Plain Ailerons at High Subsonic, Transonic, and Supersonic Speeds To Determine Some Effects of Wing Sweepback, Taper, Aspect Ratio, and Section Thickness Ratio. NACA RM L7F30, 1947.
4. Fields, E. M., and Strass, H. Kurt: Free-Flight Measurements at Mach Numbers From 0.7 to 1.6 of Some Effects of Airfoil-Thickness Distribution and Trailing-Edge Angle on Aileron Rolling Effectiveness and Drag for Wings With 0° and 45° Sweepback. NACA RM L51G27, 1951.
5. Piland, Robert O.: Summary of the Theoretical Lift, Damping-in-Roll, and Center-of-Pressure Characteristics of Various Wing Plan Forms at Supersonic Speeds. NACA TN 1977, 1949.
6. McDevitt, John B.: A Correlation by Means of the Transonic Similarity Rules of the Experimentally Determined Characteristics of 22 Rectangular Wings of Symmetrical Profile. NACA RM A51L17b, 1952.
7. DeYoung, John: Theoretical Antisymmetric Span Loading for Wings of Arbitrary Plan Form at Subsonic Speeds. NACA Rep. 1056, 1951. (Supersedes NACA TN 2140.)

TABLE I.- GEOMETRIC AND STRUCTURAL PARAMETERS

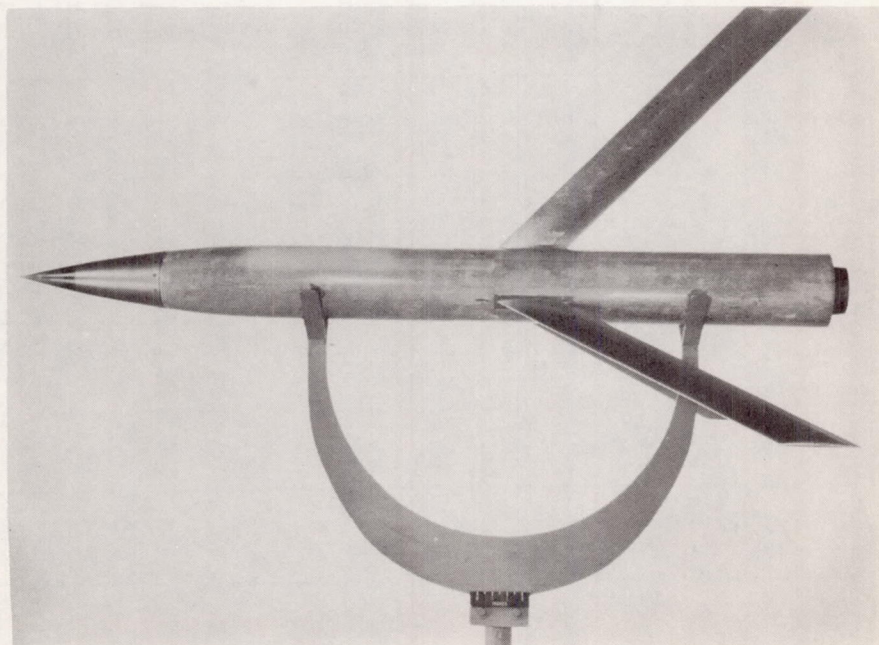
Configuration	A	Λ , deg	λ	NACA airfoil section	c_a/c	Aileron location	Type of construction	$\frac{c^4}{GJ}$	$\frac{GJ}{EI}$	Reference
1	2.3	0	1.0	^a 65-009	0.2	Full span	Composite	0.0063	1.00	3
2	2.3	45	1.0	65A009	.2	Full span	Composite	.0063	1.00	Unpublished
3	2.9	0	1.0	65A009	.2	Full span	Composite	.0056	1.03	Unpublished
4	2.9	45	1.0	65A009	.2	Full span	Composite	.0056	1.03	Unpublished
5	3.7	0	1.0	65A003	.2	Full span	Aluminum alloy	.0556	1.45	1
6	3.7	0	1.0	65A006	.2	Full span	Composite	.0130	1.14	Unpublished
7	3.7	0	1.0	65A009	.2	Full span	Composite	.0067	1.04	1
8	3.7	0	1.0	65 ₁ A012	.2	Full span	Composite	.0029	.96	Unpublished
9	3.7	45	1.0	65A006	.2	Full span	Composite	.0130	1.14	Unpublished
10	3.7	45	1.0	65A009	.2	Full span	Composite	.0067	1.04	1
11	3.7	45	1.0	65 ₁ A012	.2	Full span	Composite	.0029	.96	Unpublished
12	5.0	0	1.0	65A009	.2	Full span	Aluminum alloy	.0023	1.45	Unpublished
13	8.0	45	1.0	65A009	.2	Full span	Aluminum alloy	.0023	1.45	Unpublished
14	8.0	45	1.0	65 ₁ A012	.2	Full span	Composite	.0030	.85	1
15	8.0	45	1.0	65 ₁ A012	.2	Full span	Aluminum alloy	.0010	1.45	1
16	8.0	45	1.0	65 ₁ A012	.2	Outboard 1/2 span	Aluminum alloy	.0010	1.45	Unpublished
17	8.0	45	1.0	65 ₁ A012	.2	Inboard 1/2 span	Aluminum alloy	.0010	1.45	Unpublished
18	8.0	45	.5	65 ₁ A012	.2	Full span	Composite	.0030	.85	1
19	8.0	45	.5	65 ₁ A012	.2	Full span	Aluminum alloy	.0010	1.45	Unpublished
20	8.0	45	.5	65 ₁ A012	.2	Full span	Steel	.0004	1.43	1
21	8.0	45	.5	65 ₁ A012	.2	Outboard 1/2 span	Aluminum alloy	.0010	1.45	Unpublished
22	8.0	45	.5	65 ₁ A012	.2	Inboard 1/2 span	Aluminum alloy	.0010	1.45	Unpublished

^aNominal (see text).



(a)

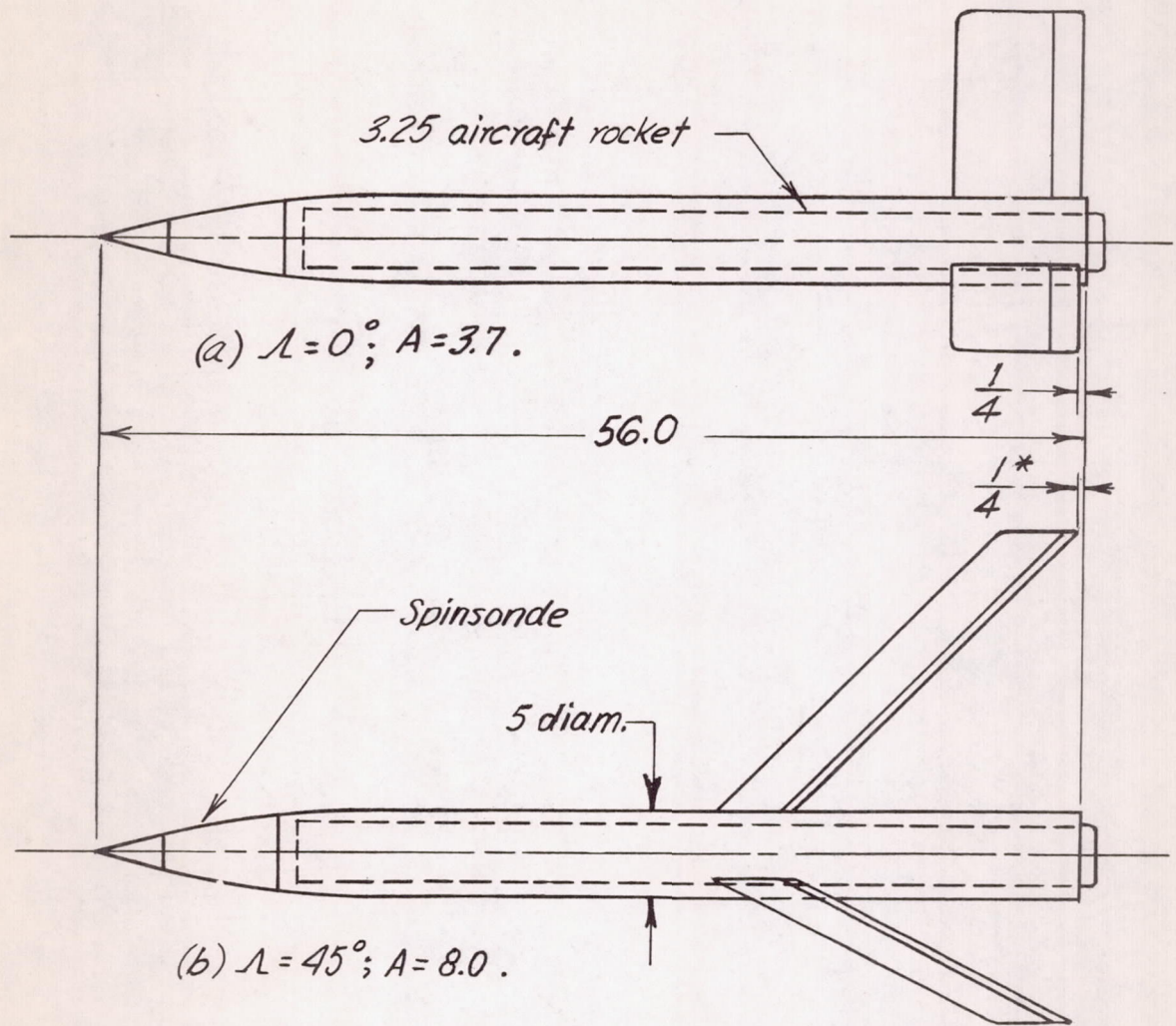
L-65634.1



(b)

L-69353.1

Figure 1.- Typical test vehicles.



* Constant for all configurations.

Figure 2.- General arrangement of typical test vehicles with NACA 65A0XX airfoil sections parallel to model center line. All dimensions are in inches.

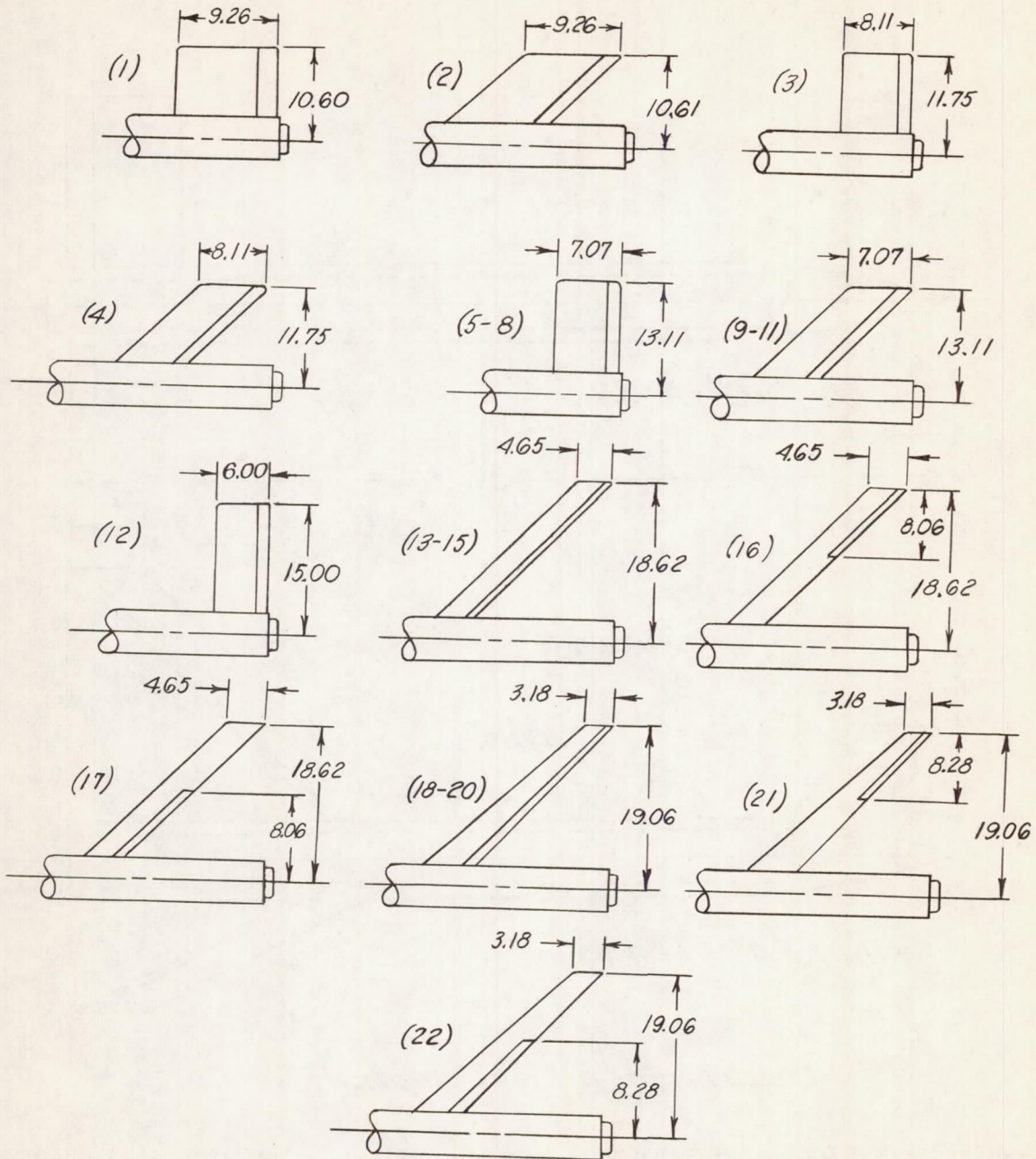
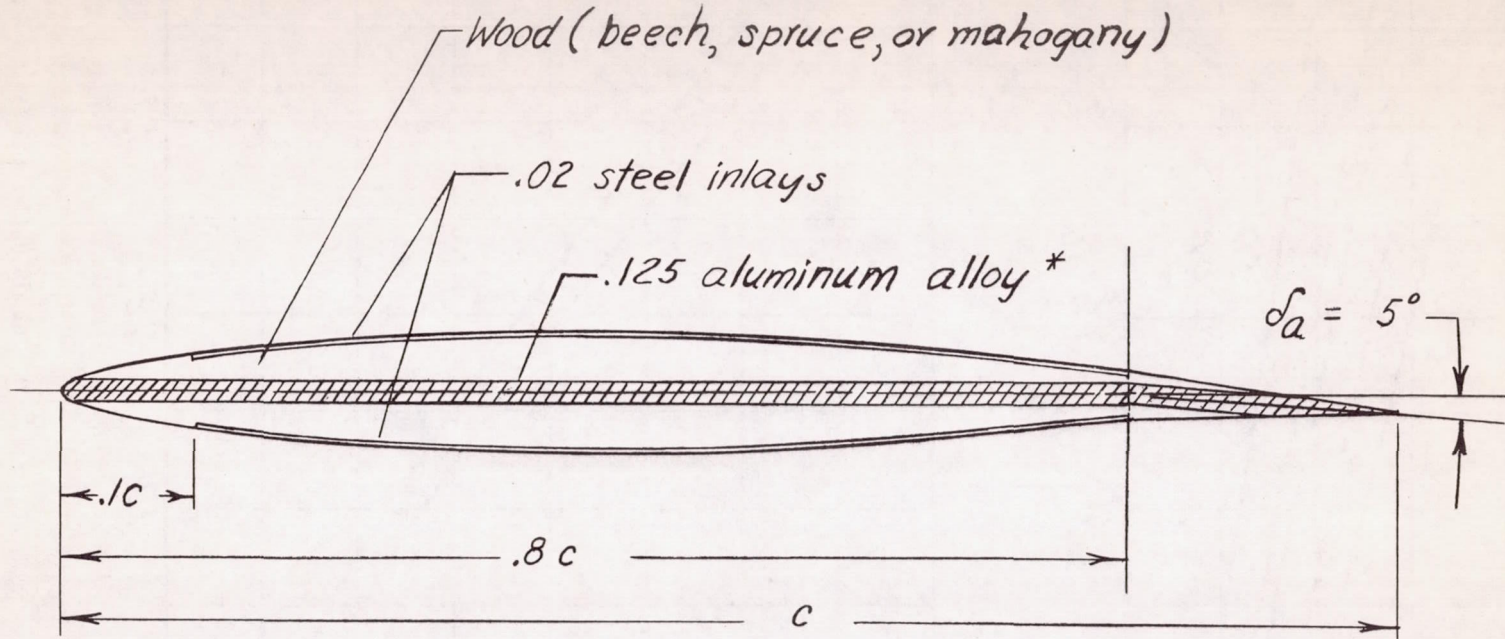


Figure 3.- Description of test wings. Exposed wing area, 75 square inches; for sweptback wings, $\Lambda = 45^\circ$. Numbers in parentheses denote configurations (see table I). All dimensions are in inches.



* Omitted in test vehicles with $A = 2.3$ and 3.7 .

Figure 4.- Typical construction of composite wings. The section is taken parallel to the model center line. All dimensions are in inches.

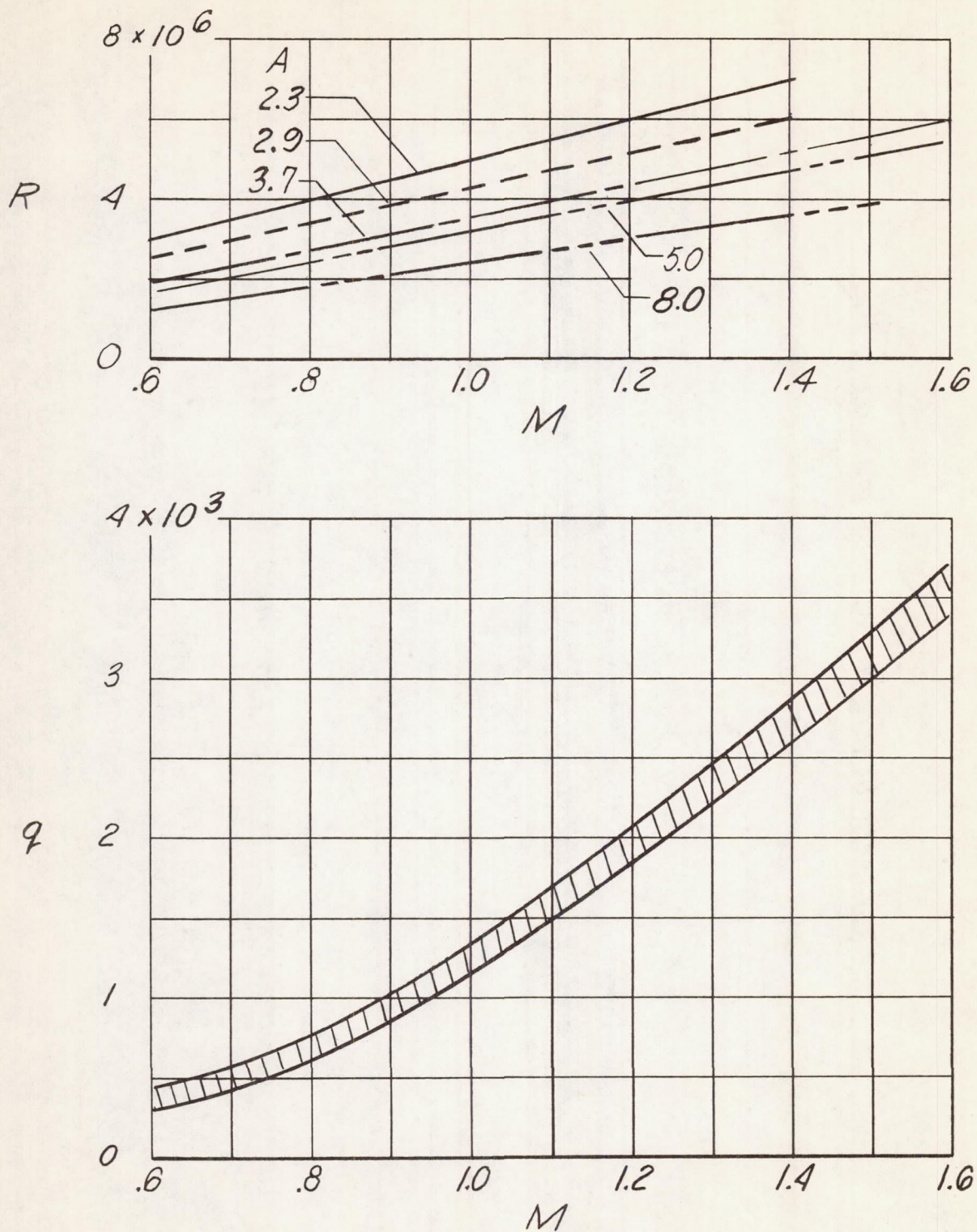


Figure 5.- Variation of Reynolds number and dynamic pressure with Mach number.

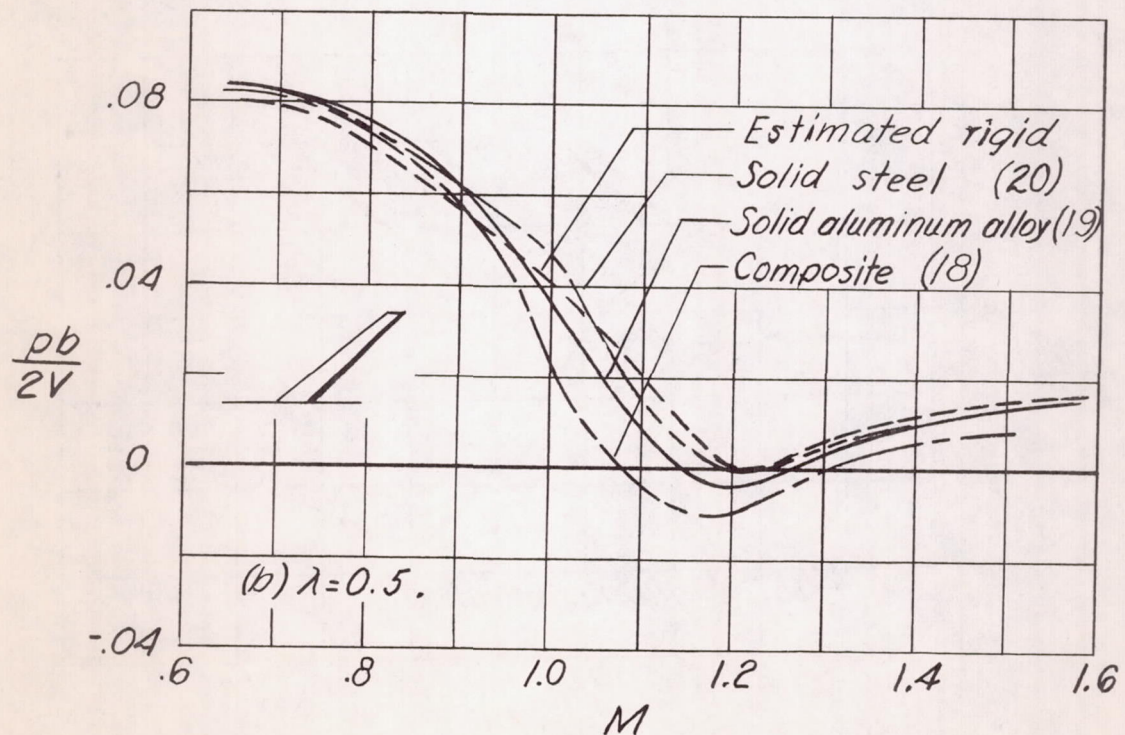
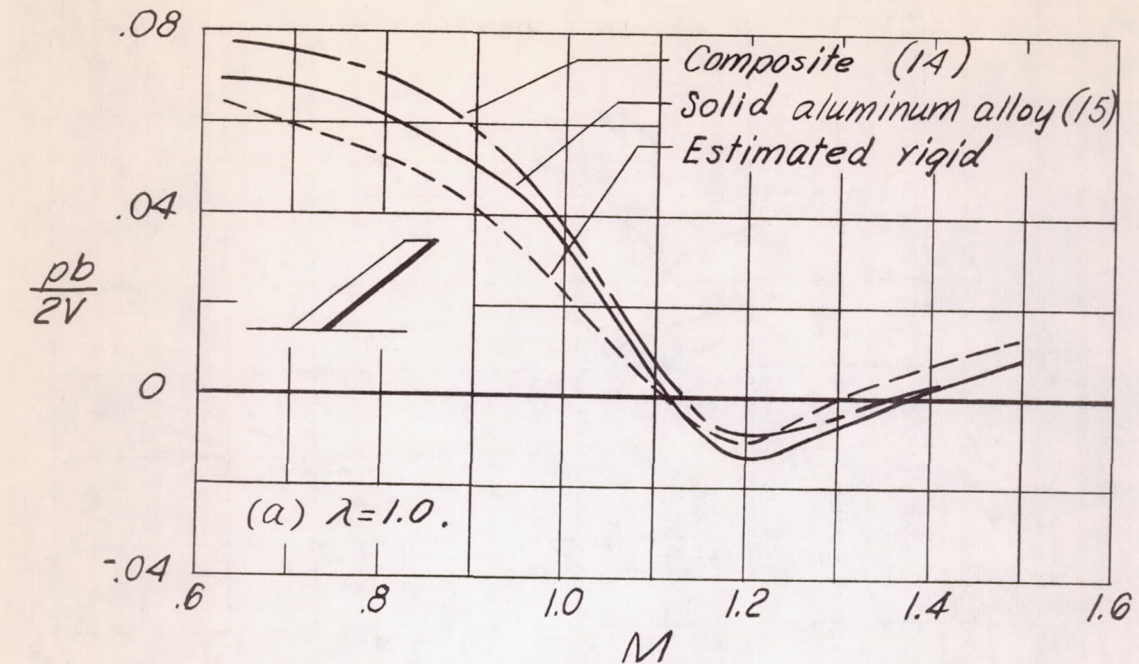


Figure 6.- Effect of wing flexibility on aileron rolling effectiveness. $A = 8.0$; $\delta_a = 5.0^\circ$; $c_a/c = 0.2$; full-span ailerons; NACA 65₁A012 airfoil sections. Numbers in parentheses denote test configurations.

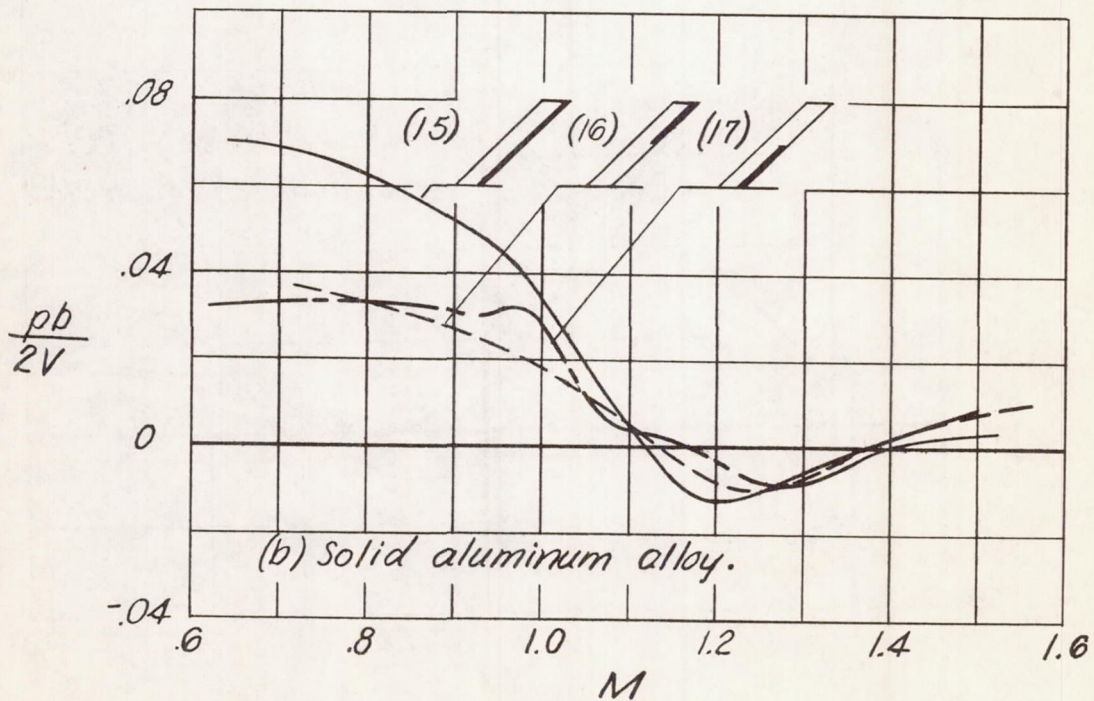
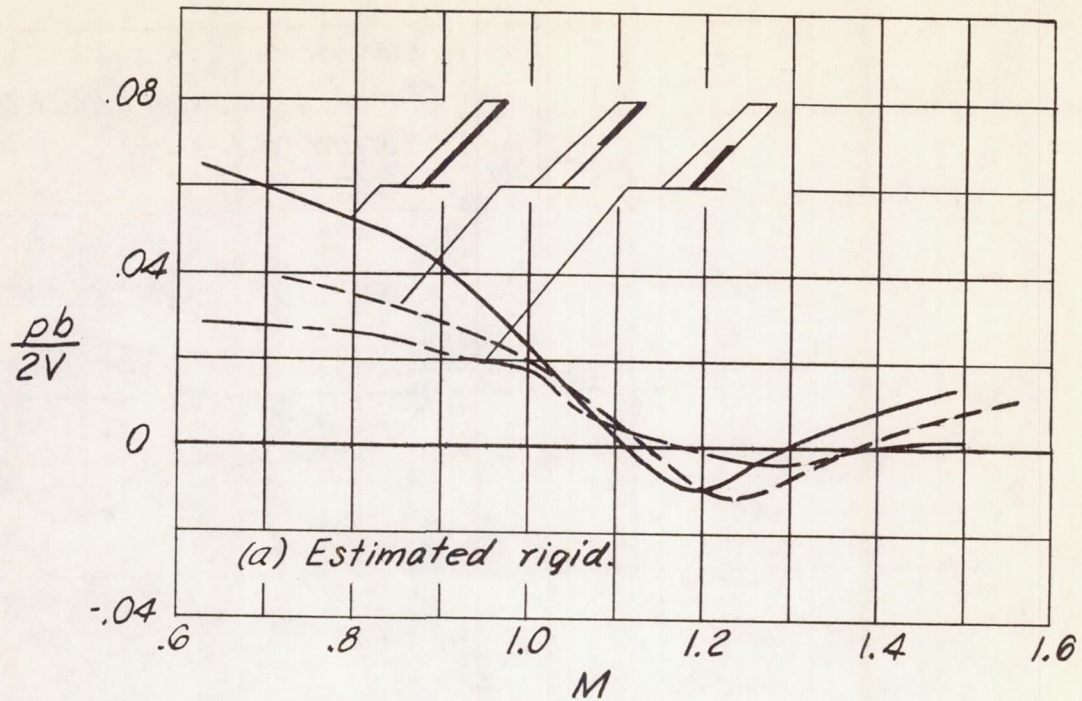


Figure 7.- Effect of aileron location on rolling effectiveness. $A = 8.0$;
 $\lambda = 1.0$; $\delta_a = 5.0^\circ$; $c_a/c = 0.2$; NACA 65₁A012 airfoil sections. Numbers
 in parentheses denote test configurations.

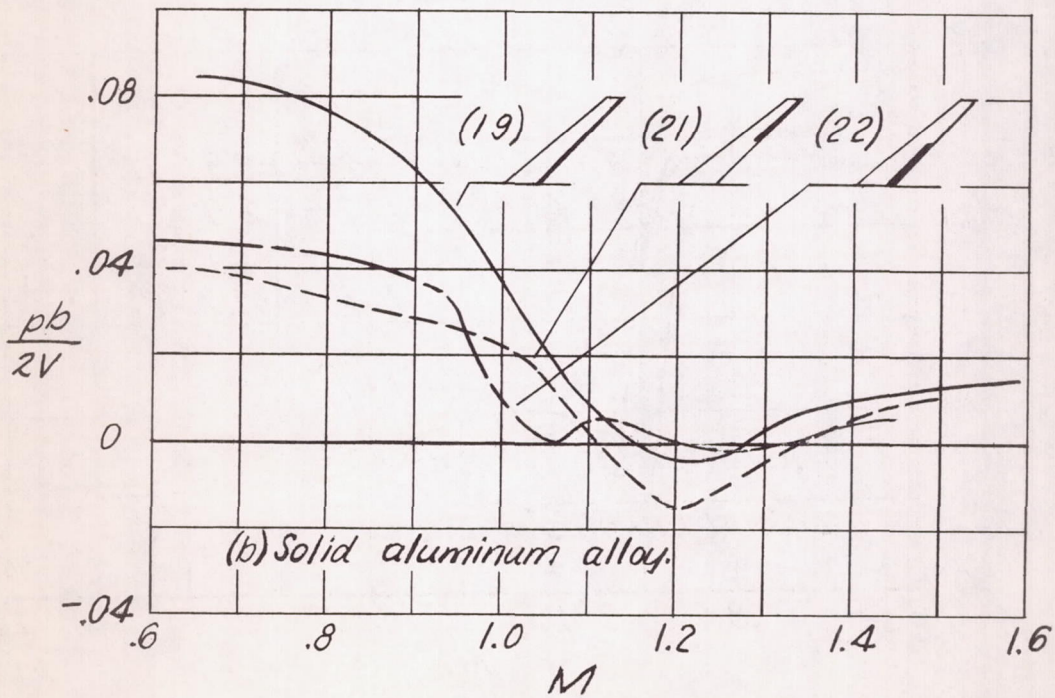
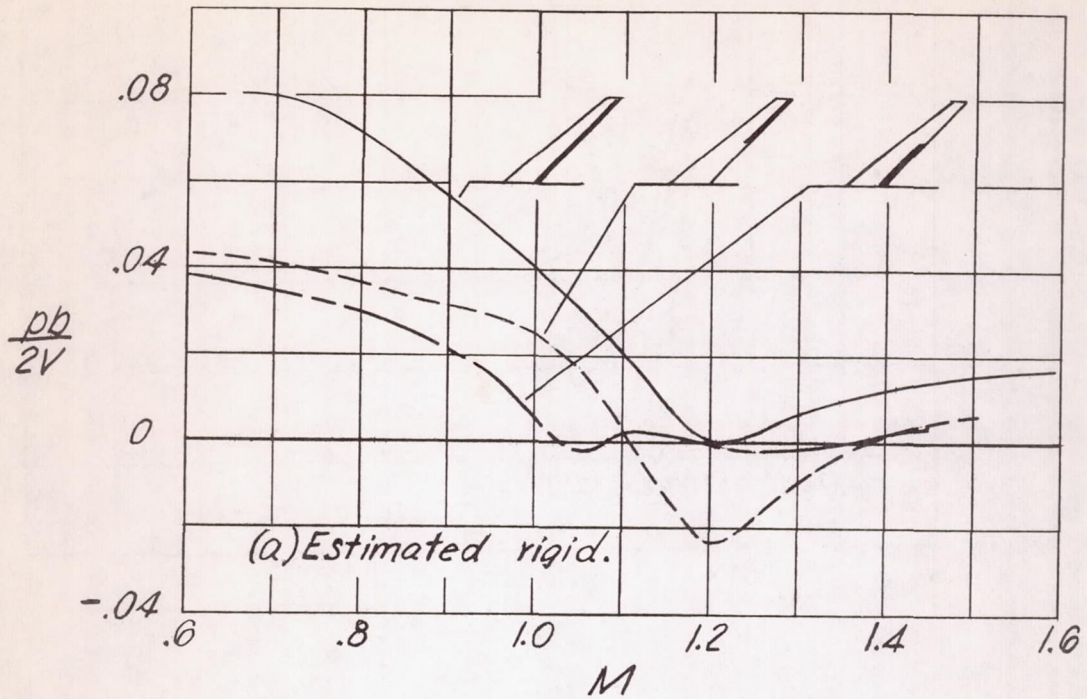


Figure 8.- Effect of aileron location on rolling effectiveness. $A = 8.0$; $\lambda = 0.5$; $\delta_a = 5.0^\circ$; $c_a/c = 0.2$; NACA 65₁A012 airfoil sections. Numbers in parentheses denote test configurations.

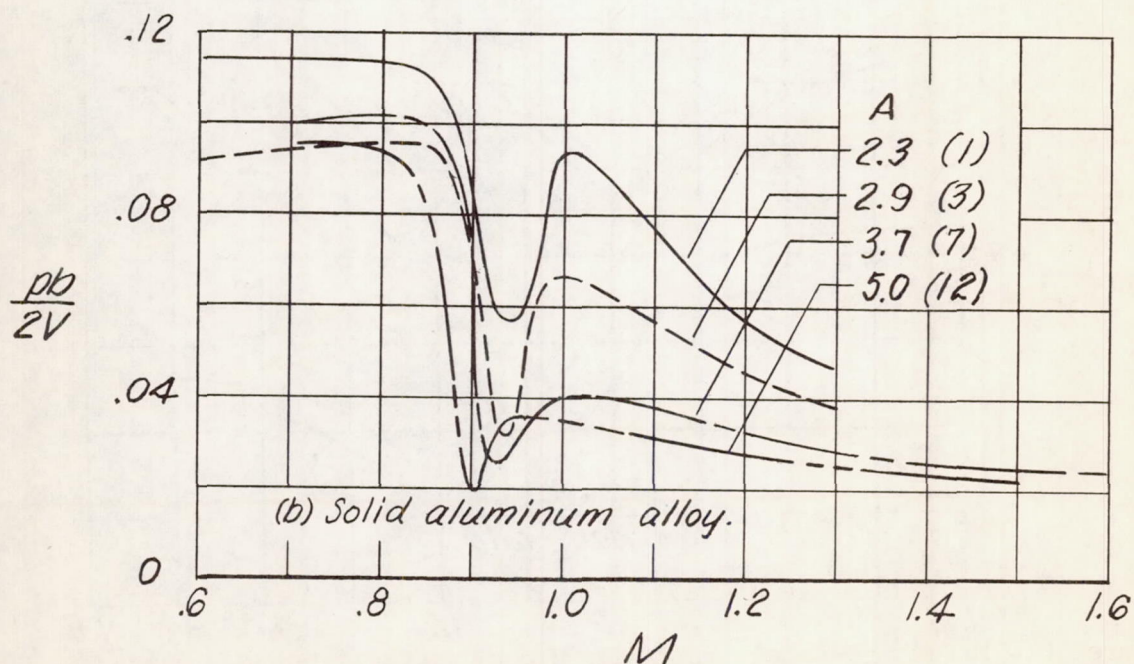
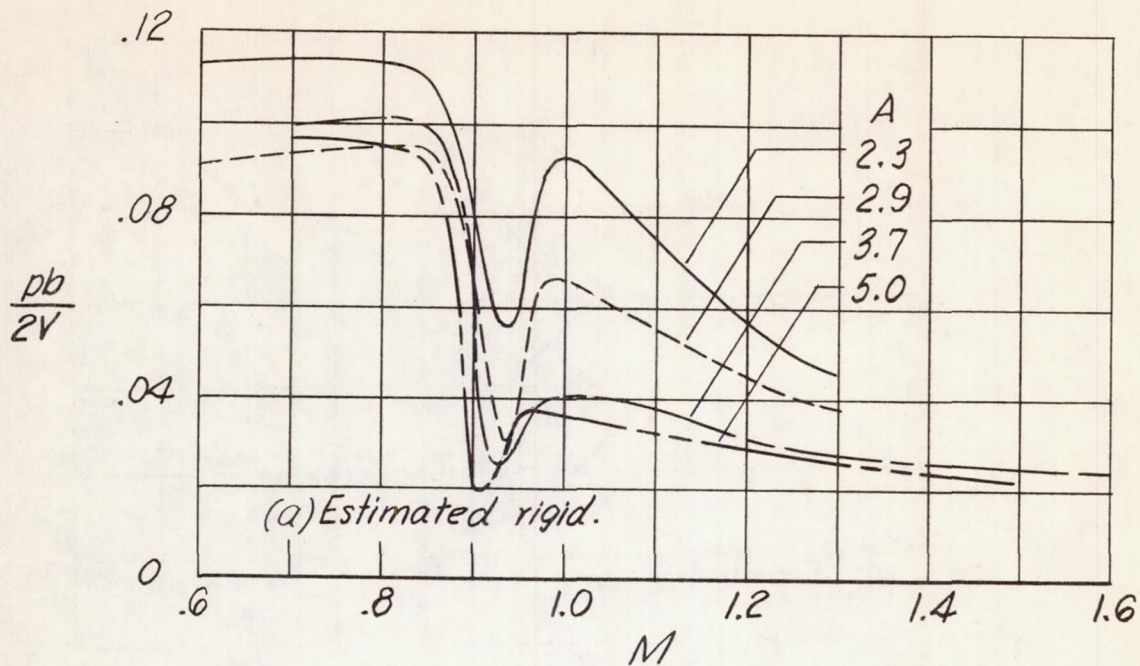


Figure 9.- Effect of aspect ratio on rolling effectiveness. $\Lambda = 0^\circ$;
 $\lambda = 1.0$; $\delta_a = 5.0^\circ$; $c_a/c = 0.2$; full-span ailerons; NACA 65A009 airfoil
sections. Numbers in parentheses denote test configurations.

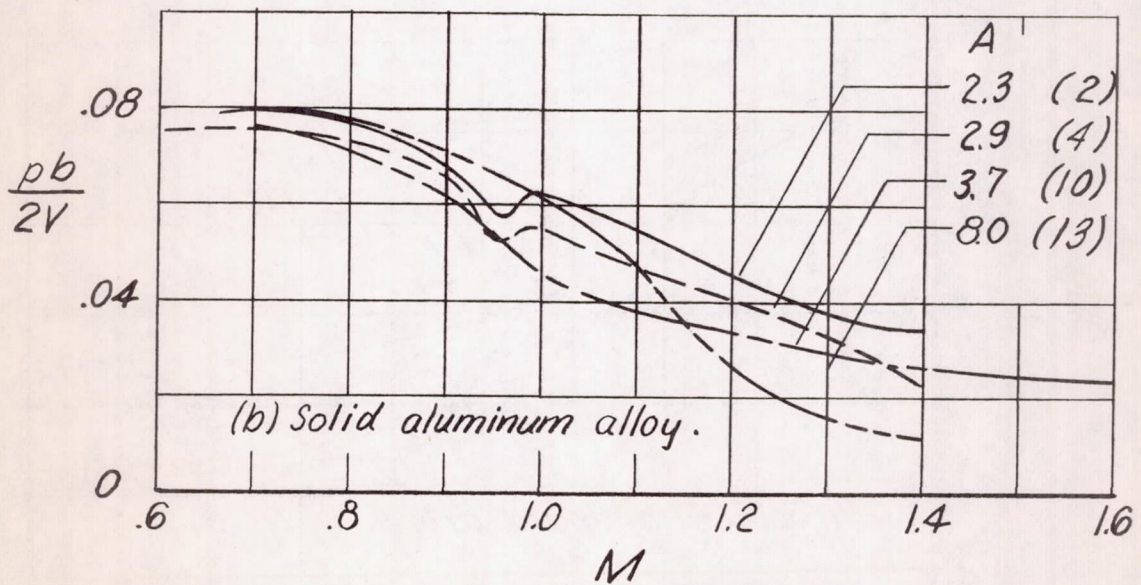
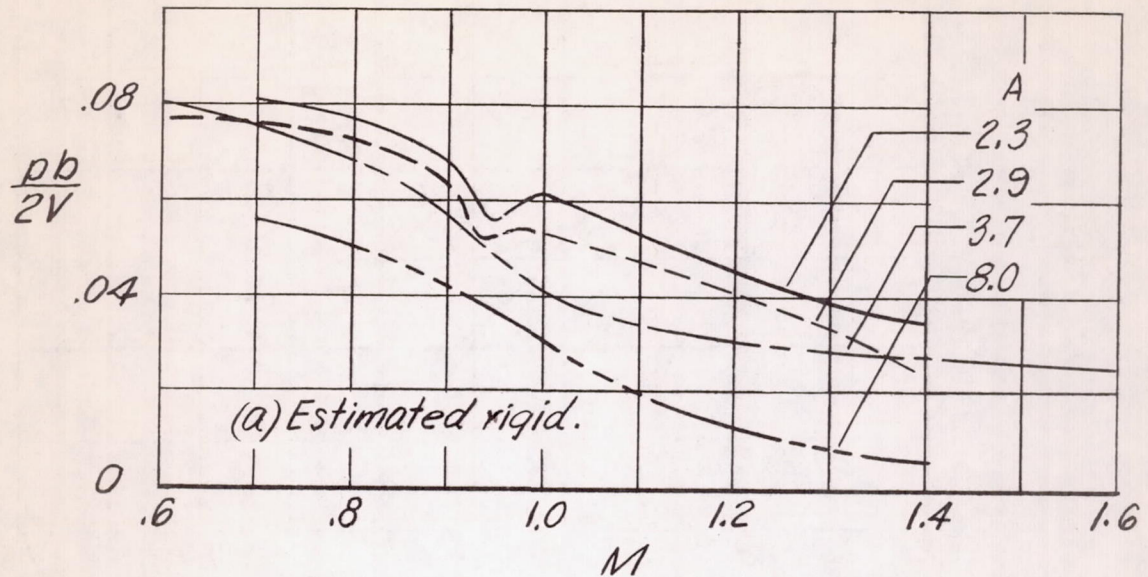


Figure 10.- Effect of aspect ratio on rolling effectiveness. $\Lambda = 45^\circ$; $\lambda = 1.0$; $\delta_a = 5.0^\circ$; $c_a/c = 0.2$; full-span ailerons; NACA 65A009 airfoil sections. Numbers in parentheses denote test configurations.

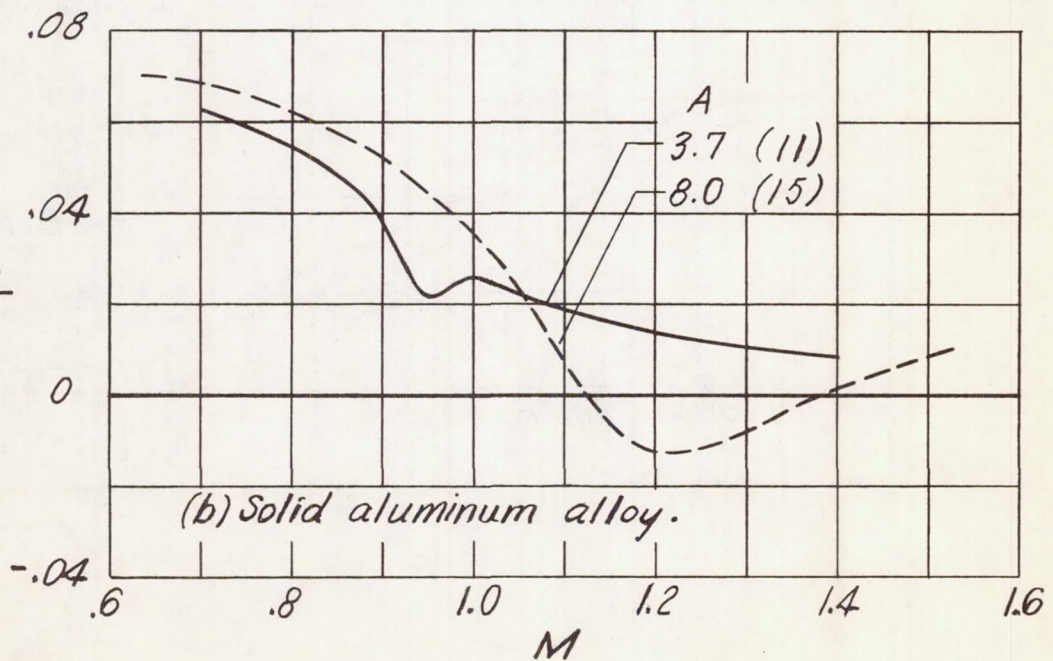
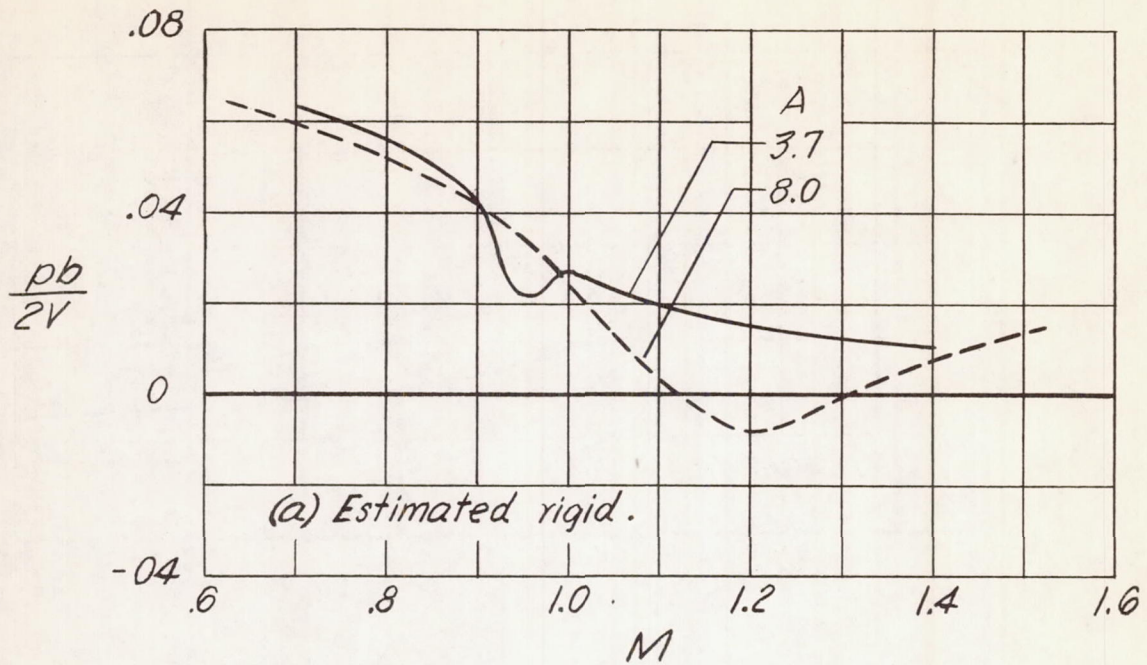


Figure 11.- Effect of aspect ratio on rolling effectiveness. $\Lambda = 45^\circ$; $\lambda = 1.0$; $\delta_a = 5.0^\circ$; $c_a/c = 0.2$; full-span ailerons; NACA 65₁A012 airfoil sections. Numbers in parentheses denote test configurations.

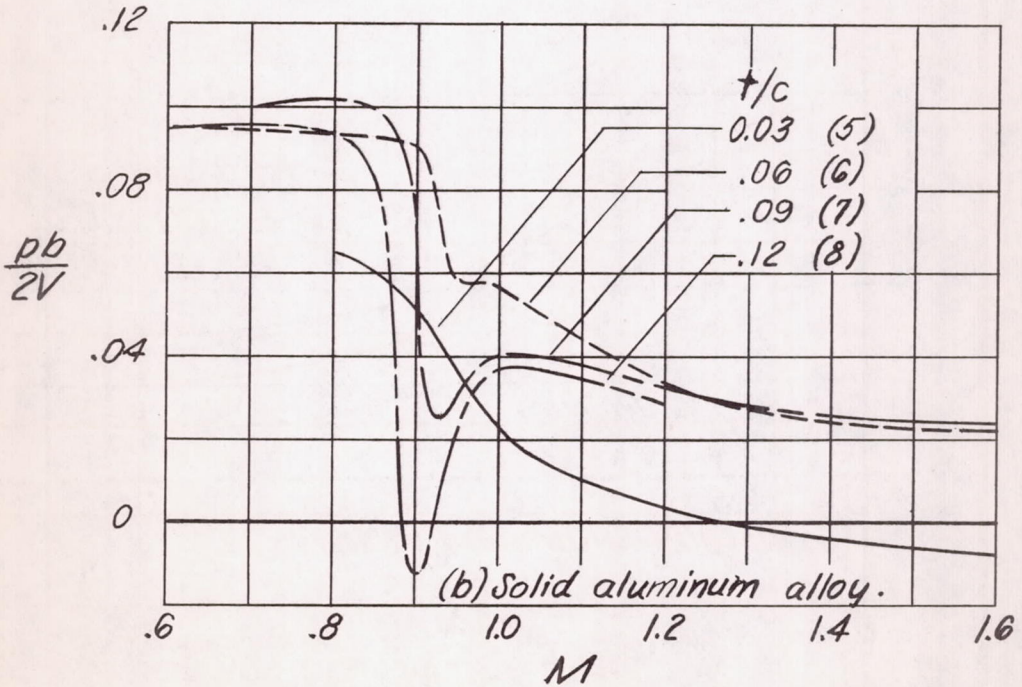
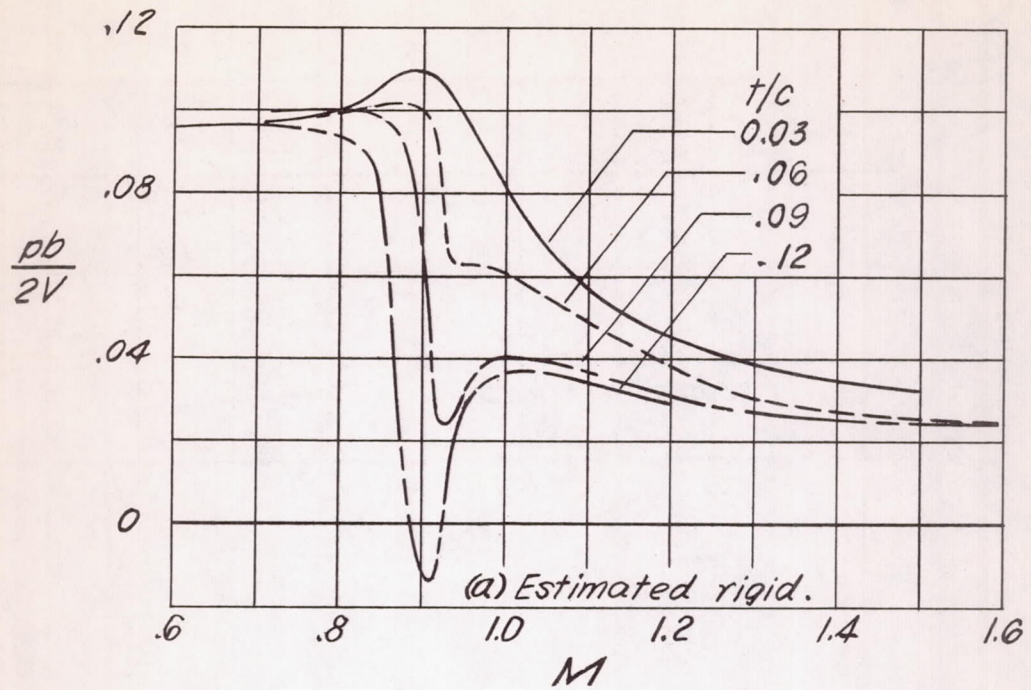


Figure 12.- Effect of thickness on rolling effectiveness. $A = 3.7$; $\Lambda = 0^\circ$; $\lambda = 1.0$; $\delta_a = 5.0^\circ$; $c_a/c = 0.2$; full-span ailerons; NACA 65A0XX airfoil sections. Numbers in parentheses denote test configurations.

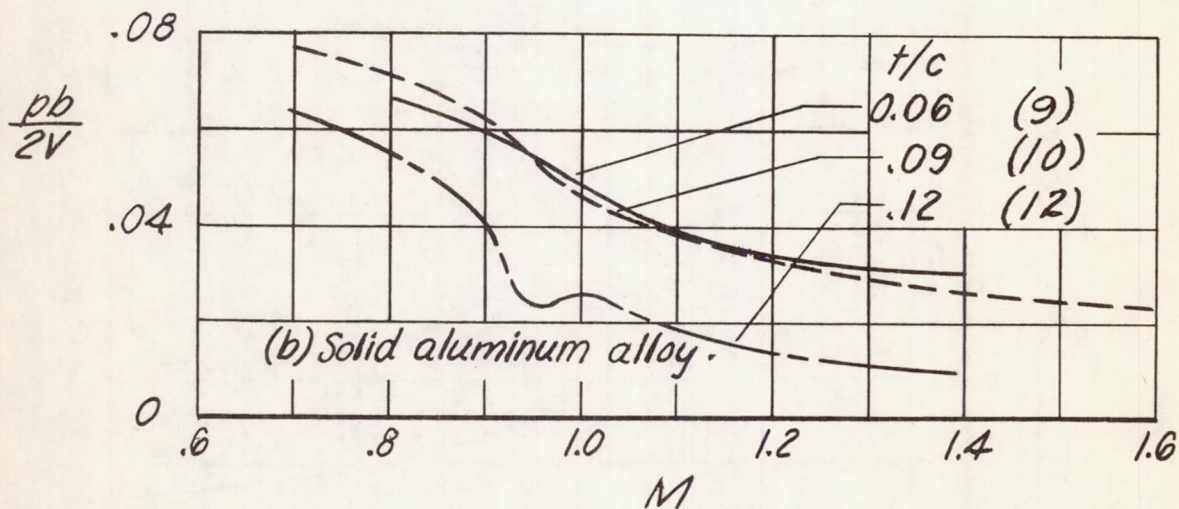
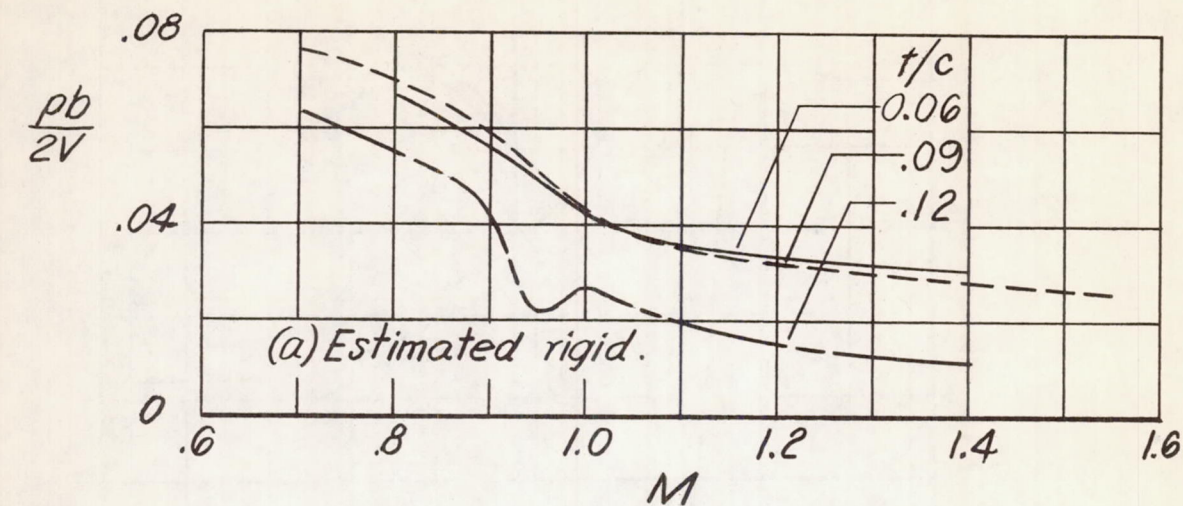


Figure 13.- Effect of thickness on rolling effectiveness. $A = 3.7$; $\Lambda = 45^\circ$; $\lambda = 1.0$; $\delta_a = 5.0^\circ$; $c_a/c = 0.2$; full-span ailerons; NACA 65A0XX airfoil sections. Numbers in parentheses denote test configurations.

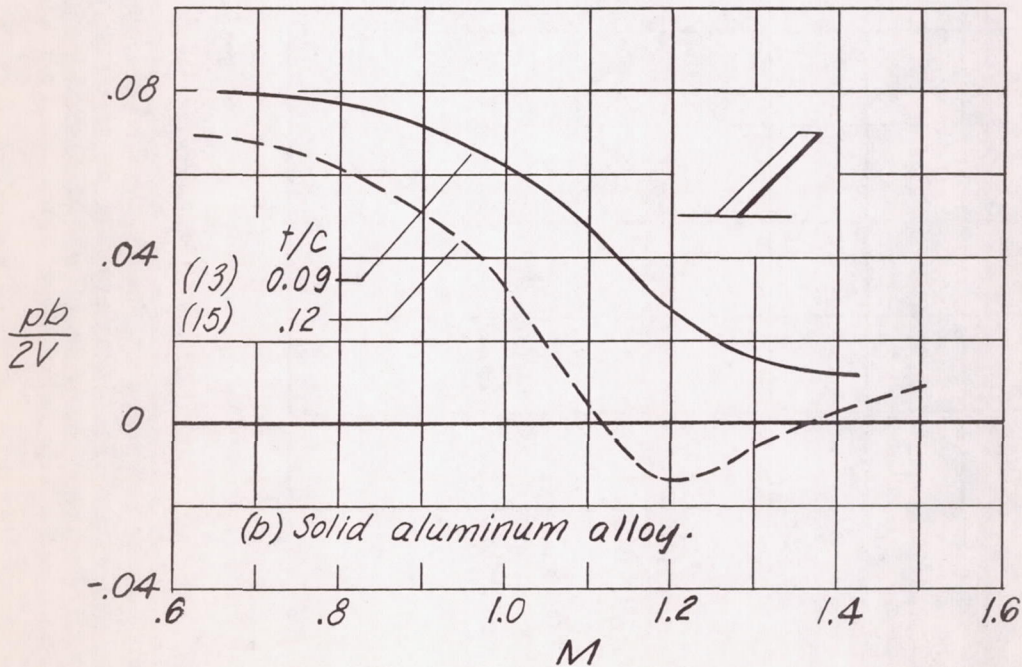
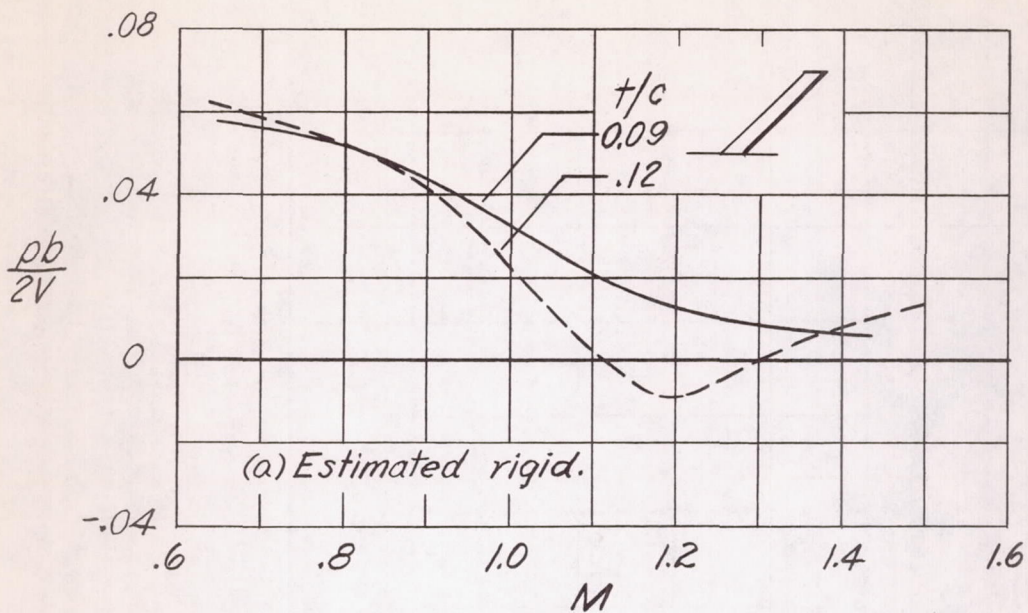


Figure 14.- Effect of thickness on rolling effectiveness. $A = 8.0$; $\Lambda = 45^\circ$; $\lambda = 1.0$; $\delta_a = 5.0^\circ$; $c_a/c = 0.2$; full-span ailerons; NACA 65A0XX airfoil sections. Numbers in parentheses denote test configurations.

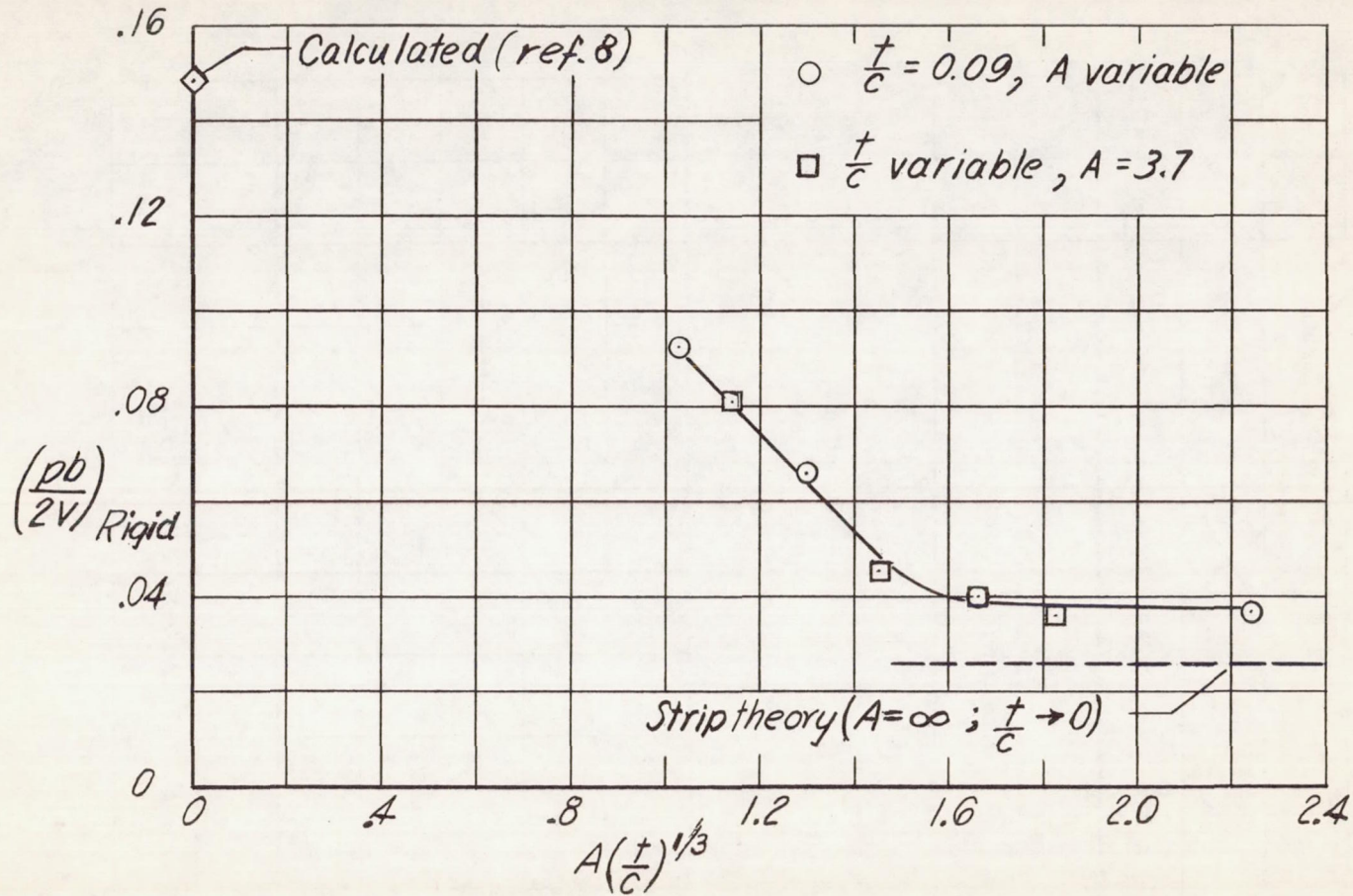


Figure 15.- Correlation of the rolling effectiveness at $M = 1.0$ of various unswept wing-aileron configurations with the transonic aspect-ratio-thickness parameter. $\delta_a = 5.0^\circ$; $c_a/c = 0.2$; NACA 65A0XX airfoil sections. Data taken from figures 9 and 12.

CONFIDENTIAL

CONFIDENTIAL